Journal of Applied Veterinary Sciences, 9 (2): 111-119 (April, 2024).
ISSN: Online: 2090-3308, Print: 1687-4072
Journal homepage : https://javs.journals.ekb.eg

Impact of Fabricated Coral Shell Hydroxyapatite Powder and Autologous Plasma Rich- fibrin in Remodeling of the Mandibular Bone Critical Size Defect in Dogs: Histopathological and Immunohistochemical Study

Ali Ghazi Atiyah[1] and Alkattan L.M[2*]
[1]Department of Surgery and Obstetrics, College of Veterinary Medicine, University of Tikrit, Iraq
[2]Department of Surgery and Theriogenology, College of Vet., Med., University of Mosul, Iraq
*__Corresponding Author:__ Alkattan L.M., **E-Mail:** laythalkattan@uomosul.edu.iq

ABSTRACT

Histopathological and immunohistochemical assessment of fabricated coral shell hydroxyapatite (CSHA) and plasma rich fibrin (PRF) in remodeling of the induced critical size defect of the mandibular bone in the dogs: Twenty-seven adult dogs of both sexes were included and equally divided into three equal groups: control, plasma-rich fibrin (PRF) and hydroxyapatite group (CSHA). The experimental mandibular bone defect was induced in a circular shape, and the dimensions of the defect were 14×5mm. Evaluation of the healing progress of the defect and associated macroscopical, histopathological, and Immunohistological findings was recorded in all studied groups at 7, 15, and 30 days post-operatively. Macroscopically, the healing was evaluated by the presence of new bone tissue filling the bone gap defect in all groups during different follow-up periods. In the plasma-rich fibrin (PRF) group, the gap was highly filled with hard, firm tissues that filled all borders and the centre of the induced gap in comparison with the coral shell hydroxyl apatite group (CSHA), which is partially filled with hard tissue. Histopathologically, the progress of healing in the PRF group was represented by the presence of highly mature connective tissue and new woven bone formation at seven days and well-developed mature bone inside defective bone at 15 and 30 days post-operatively, whereas in the CSHA group, the results were represented by the occlusion of highly mature connective tissue and new woven bone formation inside the induced hole at 15 and 30 days post-operatively. At 30 days post-surgery, in the control group, there was the presence of newly formed woven bone surrounded by the edge of the mandible bone. The immunohistochemical expression of the alkaline phosphatase (ALP) in the mandible bone at 30 days PS in the control group was represented by weak positive expression, while mild positive expression was indicated in the CSHA group and moderate positive expression in the PRF group. In conclusion, this research exhibited the role of both CSHA and PRF in improving the healing process of defective mandible bones, with a clear superiority of the beneficial value of using PRF. The histopathological and immunohistochemistry assessments emphasize these results.

Original Article:
DOI: HTTPS://DX.DOI.ORG/10.21608/JAVS.2024.266431.1312
Received : 30 Januay, 2024.
Accepted :10 March, 2024.
Published in April, 2024.

Keywords: Coral shell, Dog, Immunohistochemistry, Mandibular defect, PRF.

J. Appl. Vet. Sci., 9 (2): 111-119

INTRODUCTION

Maxillofacial defects are a challenge for many surgeons and may be traumatic, congenital, neoplastic, or iatrogenic, such as cancer ablation (**Kalantar and Khorvash, 2006**.). A critical-size bone defect refers to a bone defect that cannot heal spontaneously during an expected time of normal bone healing (**Jin *et al.*, 2005**). The animal life period in most research depends upon the end of the study; a critical-size bone defect is also determined as the smallest size of a fracture defect that does not spontaneously heal without treatment in a particular lifetime (**Marei *et al.*, 2007**). Biomaterials have a crucial role in repairing bone defects by providing the essential matrix for the differentiation and proliferation of bone cells and improving cell function (**Gao *et al.*, 2017**). They are also termed bone substitutes (**Shadjou and Hasanzadeh, 2015**). The perfect bone substitute biomaterials should be safe, non-carcinogenic, and non-inflammatory or immune rejection response, with minimal fibrosis (**Abdulghani and Mitchell, 2019**). Recently, there has been a

growing need for bone substitutes as bioactive agents, which must produce essential properties for tissue integrity, such as bioactivity, biocompatibility, and biodegradability (**Haugen *et al.*, 2019**). Various osteogenic bioactive agents are accessible for reconstructing mandibular defects in aesthetic surgery. Critical-size bone defects serve as an excellent model for evaluating the efficacy of treatments because regeneration of bone in a critical bone defect solely takes place in the presence of an osteogenic bioactive agent. (**Huh *et al.*, 2005**).

Many kinds of bone substitutes were practically used to reconstitute different types of bone defects, such as processed ribs of lamb in repairing the critical size of tibial bone in dogs (**Felipe *et al.*, 2020; Mohammed *et al.*, 2022**); processed carp shell (**Atiyh, 2018**); and processed waste eggshell (**Zebon *et al.*, 2020**). PFR, termed bioactive materials, is used as a surgical supplement to various surgical operations such as reconstruction of induced radial bone fractures in dogs (**Mohammed *et al.*, 2023**), repairing abdominal hernias in rams (**Zedan *et al.*,2022**) for acceleration, and improving bone tissue regeneration and wound healing processes (**Chandran, and Sivadasb, 2014).** PRF is a natural bioactive scaffold formed after tissue damage. It supplies the initial valuable matrix for cell adhesion, remodelling properties, tissue differentiation, and proliferation (**Allawi *et al.*, 2019**; **Zedan *et al.*, 2023**).

Recently, platelet-rich fibrin (PRF) was used in oral surgery for both humans and dogs to promote tissue healing and regeneration. (**Tambella *et al.*, 2020**). The objective of this work is to assess the histopathological and immunohistochemical properties of fabricated coral shell hydroxyapatite and plasma-rich fibrin in remodelling the defect-induced mandibular bone in dogs.

MATERIALS AND METHODS

Animals and study design

This study was approved by the ethical committee at the Faculty of Veterinary Medicine, Mosul University, Iraq (UM.VET.2022.050). All dogs were treated following guidelines established by the international and institutional Animal Care and Use Committees.

Twenty-seven healthy adult Mongrel-intact dogs of both sexes were included in the present study. The mean age enrolled was 1.6±0.4 years and weighed 18 ± 0.8kg, respectively. Before inclusion, all dogs underwent a complete physical and clinical examination to ensure that they were completely healthy and free from infectious, contagious, or musculoskeletal diseases. All dogs underwent the same management conditions, including accommodation, feeding, and housing, at the Veterinary Medicine College/University of Mosul during the period of research from December 2022 to October 2023.

The animals were divided randomly into two equal groups of nine dogs each, according to the following:

Group 1: Only induced critical size of the mandibular defective gap without any treatment and considered as the Control group.

Group 2: Induced critical size of mandibular defective gap treated with fabricated coral shell hydroxyapatite (CSHA).

Group3: Induced critical size of mandibular defective gap treated with prepared PRF.

Induction of a critical size defect in the mandibular bone

A critical-size bone defect was carried out under general anesthesia. The enrolled dogs were routinely pre-medicated with 0.04 mg/kg Atropine Sulphate (Atrovap, Vapco, Jordan) given subcutaneously and anesthetized with a mixture of (5 mg/kg) 2% Xylazine HCL (Interchemie, Holland) and (10 mg/kg) 10% ketamine HCL (Alfasan, Holland) given intramuscularly in one syringe (Alkattan **and Helal, 2013**). The mandibular bone defect was induced experimentally in a circular shape with dimensions of 14 × 5 mm, respectively. In the first group, the mandible bone defect was lifted without treatment, and the subcutaneous skin was then closed routinely. In the second group (CSHA), the defect was reconstructed by using fabricated hydroxyapatite powder from the coral shell through the hydrothermal method. This powder was applied directly through the mandible bone defect, and then the subcutaneous and skin were closed routinely. In the third group (PRF), the defect was repaired by using prepared plasma-rich fibrin as a filling material, which was applied directly through the mandible bone defect. Then the subcutaneous and skin were closed routinely **(Fig.1).** Histopathological and immunohistological investigations were studied (7, 15, and 30 days).

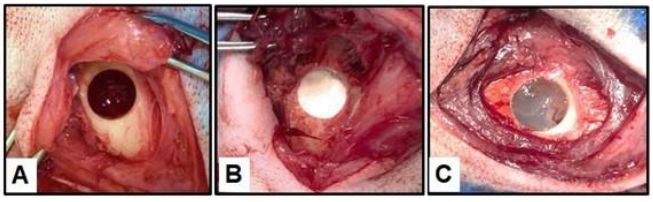

Fig.1: Image shown induced mandibular defect A: control group. B: treatment group with fabricated coral shell hydroxyapatite powder group. C, treatment group with prepared PRF group.

PRF preparation

The PRF was prepared according to (Gobbi), 10 ml of blood was collected from the dog's jugular vein, and then the blood sample was centrifuged at 3000 rpm for 10 min to obtain mid layer containing PRF matrix, this homogenous matrix was obtained and applied directly at the previously induced defect (**Gobbi and Vitale, 2012**).

Fabrication of hydroxyapatite powder from coral shell

The coral shells (Pectinidae) were collected from a local market in Basra Province, Iraq, and underwent a thorough cleaning process using distilled water. Subsequently, they were subjected to boiling in a mixture of distilled water and 70% ethanol to eliminate any residues, followed by drying in a hot air oven at 100 °C for 30 minutes. Once dried, the shells were finely ground into a powder utilizing an electrical mortar grinder (Retsch, RM200, China) (**Roudana *et al.*, 2017**). The obtained powder underwent calcination in a muffle furnace (Nabertherm, Germany) at 1200 °C for 2 hours, yielding calcium hydroxide Ca (OH)2 powder. To further process the calcium hydroxide, an orthophosphoric acid solution (Ridel, Turkey) with a 0.6-molar concentration was introduced into the Ca $(OH)_2$ solution. The pH of the reaction was meticulously adjusted to 8.5 using a pH meter. In this step, a white and homogeneous precipitate was formed. The product was left at room temperature for 48 hours . to allow the reaction to age. Followed by dried precipitation, underwent a second round of calcination at 1200°C for 2 hours. The outcome was a fine white crystalline powder, confirming the presence of hydroxyapatite (HA) crystal powder, as illustrated in **Fig. 2.**

Fig.2: Image represented fabricated coral shell hydroxyapatite powder.

Tissue collection and processing

The samples were collected from healthy and treated bone tissues in an aseptic condition. The method included using 10% neutral buffered formalin (NBF) for 72 hours to fixate the sample; the bone biopsies were decalcified by using a 10% formic acid solution for 14 days, and then the sample was embedded in paraffin wax. All the samples were sliced into 5µm using a microtome, then subsequently counterstained with hematoxylin and eosin (**Survana *et al.*, 2013**).

Immunohistochemistry (IHC) analysis

The tissue sections underwent deparaffinization, rehydration, and deactivation, and then the immunohistochemistry method used was the avidin-biotin immunoperoxidase technique. Endogenous peroxidase was blocked by a mixture of 3% hydrogen peroxide and methanol solution for 7 minutes at ambient temperature. After washing with PBS containing 0.01% thiomersal and 50% glycerol at pH 7.3, the sample was blocked with 10% normal goat serum for 30–40 minutes at ambient temperature.

Then, the slides were incubated with primary antibodies, which are Alkaline Phosphatase (ALP) Polyclonal Antibody at a 1:100 dilution (Elabscience, USA) for 24 hours at 4 °C, followed by double -imes washing oof theslides with PBS for three mminutes, then incubated with poly-HRP goat anti-rabbit IgG as a secondary antibody with a dilution of 1:400 (Wuhan Fine Biotech, China) for 30 minutes at room temperature, and finally washed again with PBS. Then, the stain was performed using the DAB system. Later, all slides were allowed to be counterstained with nuclei with hematoxylin for 30 seconds at room temperature, rinsed in distal water, then dehydrated, cleared, and mounted (**Hoshi *et al.*, 1997**).

RESULTS

The macroscopic results indicated the presence of the new bone tissue formation filled the defective areas in all groups in several respects during different periods of treatment especially at 30 days post-surgery, so in the control group, the healing was represented by the presence of fibrous tissue rather than bone tissue. Generally, more new bone tissue represented the healing process way could be observed in the PRF group, which is highly filled with hard firm tissues that filled all borders and centers of the experimentally induced gap, in comparison with the CSHA groups, which are partially filled with hard tissue **(Fig.3).**

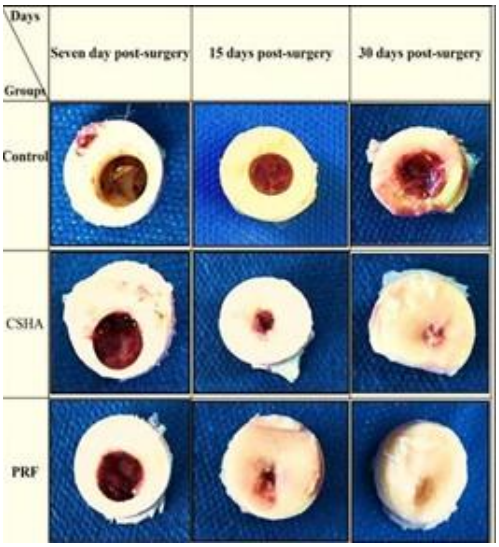

Fig.3: The progressing macroscopical healing process in control, CSHA, and PRF groups.

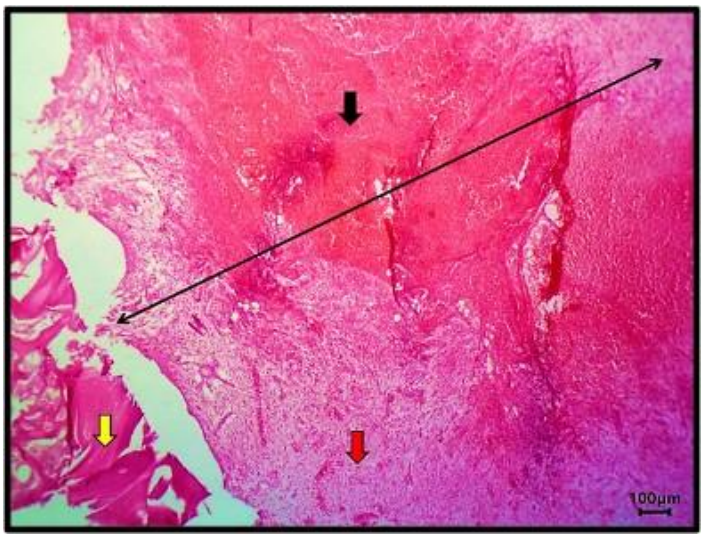

Fig.4: Histopathological section in the control group at 7 days, showing the site of hole (↔) with severe hemorrhage or blood clot (black arrow), surrounding by granulation tissue (red arrow) and the edge of the mandible bone (yellow arrow). H&E stain, 100X.

The histopathological evaluation in the control group at seven days showed the site operation had soft tissue reactions represented by severe haemorrhage with the blood clot, surrounded by a large area of granulation tissue that separated from the edge of the normal mandible bone **(Fig. 4).** At 15 days post-surgery, the results exhibited haemorrhage occlusion inside the induced hole, mature connective tissue formation, and new woven bone with newly formed blood vessels **(Fig 5).** At 30 days after surgery, the result showed that the defective area was filled with mature connective tissue rich in vascularity, and a small amount of newly formed woven bone surrounded the edge of the mandible bone defect **(Fig. 6).**

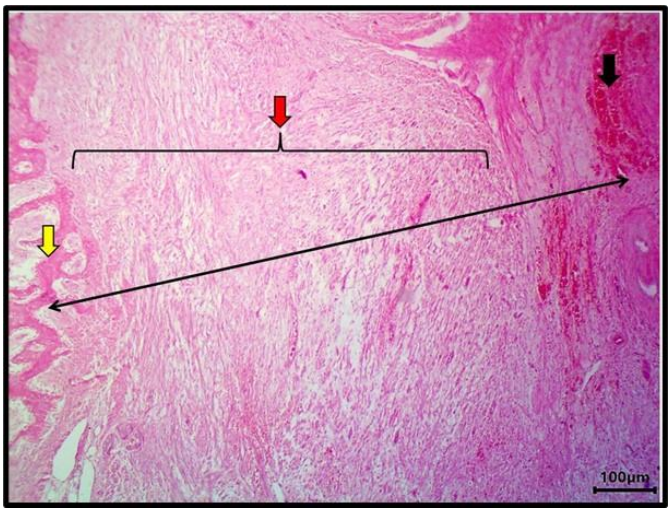

Fig.5: Histopathological image of the control group at 15 days, showing the site of the hole (↔) occluded with hemorrhage (black arrow), highly granulation tissue with high connective tissue (red arrow), and new woven bone (yellow arrow). H&E stain, 40X.

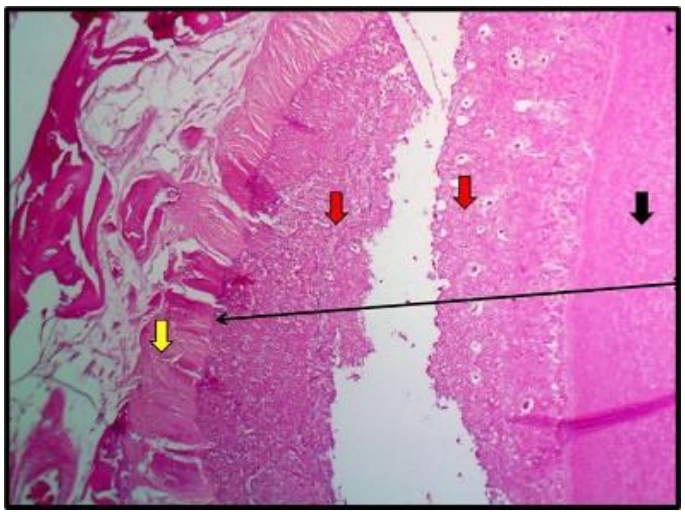

Fig. 6: histopathological image of the control group at 30 days, showing the site of hole (↔) occluded by highly mature connective tissue (black arrow) and formation of new woven bone (red arrow), with the edge of the mandible bone (yellow arrow). H&E stain, 40X.

The histological section of the mandible bone defect in the CSHA group at seven days showed the site of a hole surrounded by highly mature connective tissue and a highly new woven bone formation with high vasculature at the edge of the mandible bone **(Fig. 7).**

At 15 days after surgery, the histopathological observations of the mandibular bone defect of the CSHA group showed the site of the hole partially occluded by highly mature connective tissue, and the new woven bone formation extended from the defect margins towards the center, with the edge of the mandible bone **(Fig. 8).**

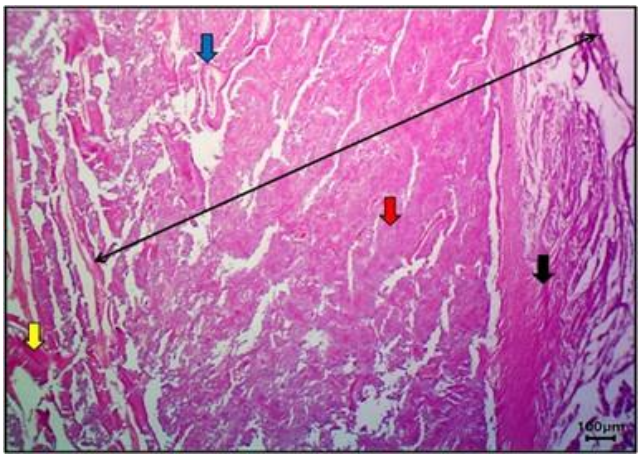

Fig.7: Histopathological image of the CSHA group at seven days, showing the site of the hole (↔) surrounded by highly mature connective tissue (black arrow), with highly new woven bone formation (red arrow) and high vasculature (blue arrow) and the edge of the mandible bone (yellow arrow), H&E stain, 40X.

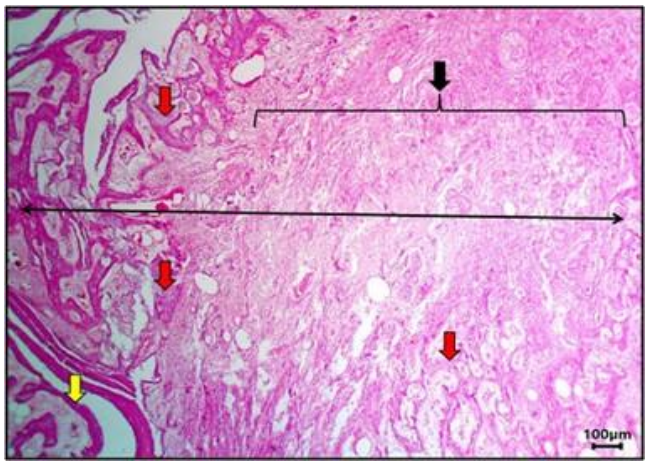

Fig.8: Histopathological section in the CSHA group at 15 days, showing the site of the hole (↔) occluded by highly mature connective tissue (black arrow) and well-developed new woven bone formation (red arrow), with the edge of the mandible bone (yellow arrow). H&E stain, 40X.

At 30 days after surgery, the histopathological observations of the CSHA group showed the site of the hole occluded by highly mature connective tissue with high vasculature and well-developed new woven bone formation with the edge of the mandible bone **(Fig. 9).** In the PRF group, at seven days, the site of the hole with the remaining PRF was surrounded by highly mature connective tissue, new woven bone formation, and the edge of the mandible bone **(Fig. 10).**

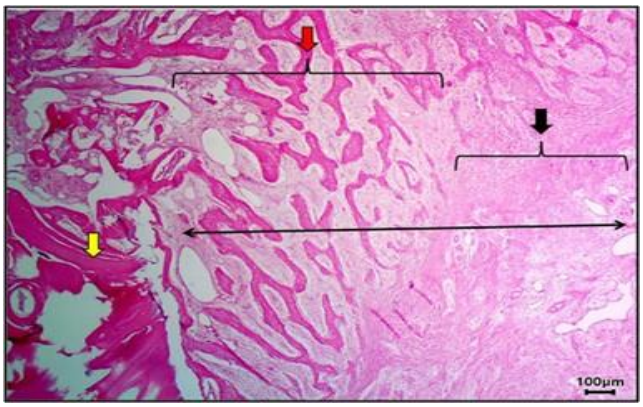

Fig.9: Histopathological image of the CSHA group at 30 days showing the site of the hole (↔) occluded by mature connective tissue (black arrow) and very well-developed new woven bone formation (red arrow), with the edge of the mandible bone (yellow arrow), H&E stain, 40X.

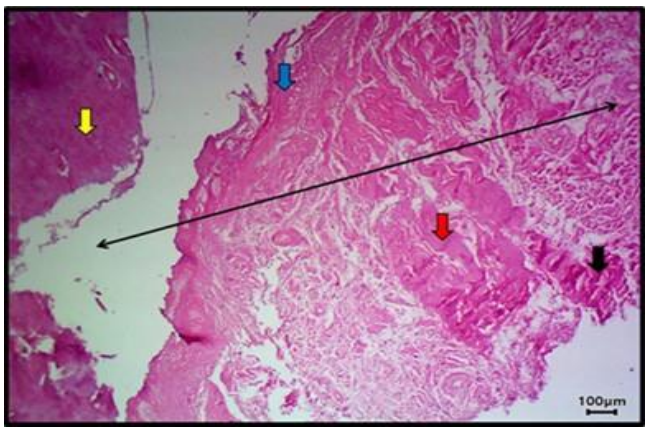

Fig.10: Histopathological image of the PRF group at seven days reveals the site of the hole (↔) with the rest of PRF (black arrow) surrounded by highly mature connective tissue (red arrow), new woven bone formation (blue arrow) and the edge of the mandible bone (yellow arrow), H&E stain, 40X.

At 15 days after surgery, there was also remaining PRF at the site of the hole, occluded by mature connective tissue, immature bone formation, and mature bone **(Fig. 11).** At 30 days after surgery, there was immature bone formation and well-developed mature bone inside the site of the defect **(Fig. 12).**

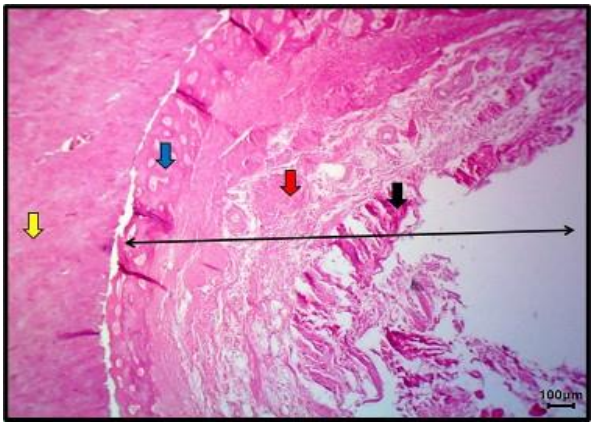

Fig. 11: Histopathological image of the PRF group at 15 days reveals the site of the hole (↔) with the rest of PRF (black arrow), occluded by mature connective tissue (black arrow) immature bone formation (red arrow), and mature bone (yellow arrow), H&E, 40X.

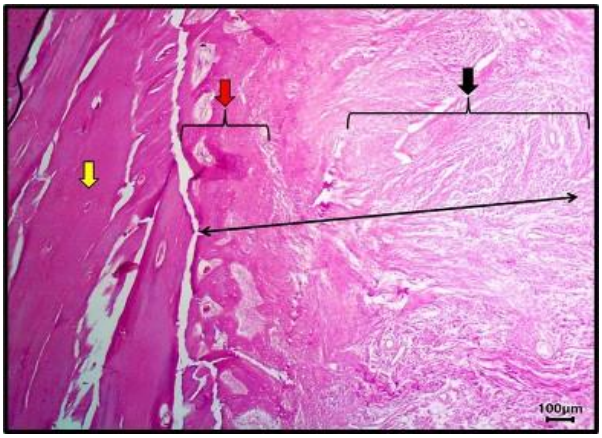

Fig.12: Histopathological image of the PRF group at 30 days reveals, the site of the hole (↔) occluded by immature bone formation (black arrow) and well-developed mature bone (red arrow), with the edge of the mandible bone (yellow arrow). H&E stain, 40X.

Immunohistochemistry

The immunohistochemical expression of the alkaline phosphatase in the mandible bone at 30 days after operation in the control group illustrated a weak positive expression **(Fig. 13).** In the CSHA group, there was a mild positive expression **(Fig. 14).** While the PRF group showed a moderately positive expression **(Fig. 15).**

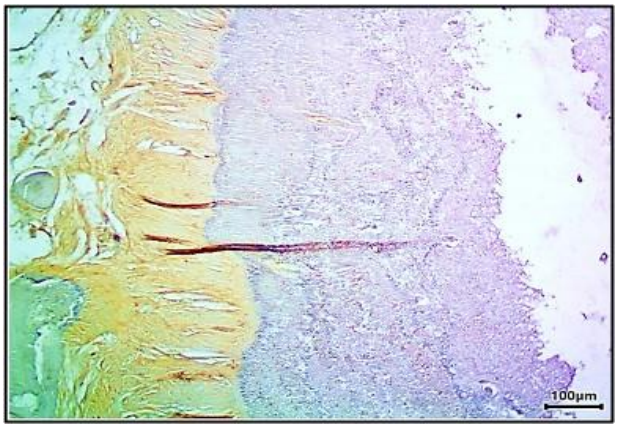

Fig.13: Immunohistochemical expression of the Alkaline Phosphatase of the mandible bone defect in the control group, observed a weak positive expression; hematoxylin stain; 100X.

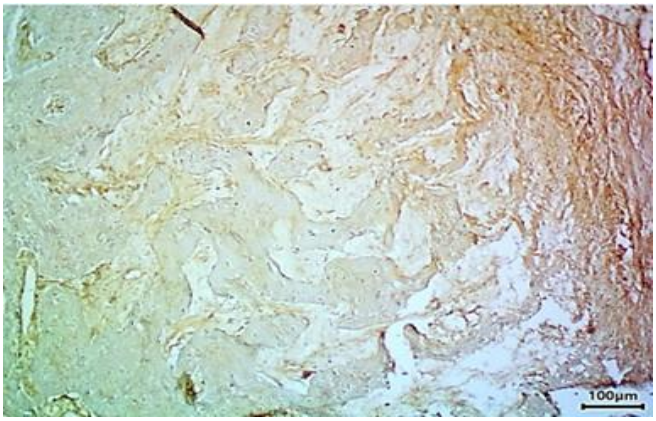

Fig.14: Immunohistochemical expression of the Alkaline phosphatase of the mandible bone defect in the CSHA group observed, a moderate positive expression; hematoxylin stain; 100X.

DISCUSSION

In this study, the surgical wounds were healed with the first intention in all groups without any signs of swelling, wound exudation, infection, or dehiscence. Therefore, we suggested that the lateral surgical approach of the mandibular bone used in this study be considered surgically under aseptic conditions and suitable for rapid exposure to the lateral border of the mandibular bone with minimal soft tissue trauma; therefore, this outcome agrees with the recent study that reported the lateral approach to the mandible in the dog was associated with fewer wound-related complications (**Cinti *et al.*, 2021**). Excessive new bone tissue in a progressing way could be visually observed in the PRF group, which is extremely filled with hard, firm tissues that filled all borders and centers of the experimentally induced gap, in comparison with the CSHA groups and control group, which are partially filled with hard tissue, and based on these outcomes, it was concluded that all bioactive materials were used in the present study to improve and enhance bone tissue formation in different clinical conditions. Therefore, our macroscopical findings agreed with previous observations that considered the use of bone substitute biomaterials stimulated osteoblast proliferation and can induce the formation of new bone with no immunological or inflammatory reaction to the bioactive material implanted in the critical-size defect gaps, and this agent has biocompatible properties **(Zhang *et al.*, 2019; Hussein and Taqa, 2021**).

As a result, histopathological sections in all groups have shown no obvious signs of tissue necrosis or abnormal cellular activity (such as

distraction of osteocytes) in the bone defective area, which indicated that no thermal production or bone crack damage occurred during the drilling force. Furthermore, osteocytes, known as the cells that sense mechanical strain in the bone matrix, are very sensitive to it. The typical appearance of osteocytes within the lacune in the native bone margin also indicated mechanically loaded force was absent in the bone during the drilling technique (**Alam *et al.*, 2019**). Also, our histopathological investigations revealed that the mandibular bone defects healed represented by endochondral rather than intramembranous bone formation because the presence of cartilage template was observed; this result was following the previous study by **Komatsu *et al.* (2009**), which illustrated that the histology of the drill bone defect models was initiated with intramembranous ossification rather than formation of the cartilage template, due to the mechanical stability of the gap defect. At this point, in the control group, there was a preponderance of soft tissue reactions at seven and 15 days after surgery. This reaction consisted of a mixture of hematoma due to severe haemorrhage and granulation tissue formation. However, in the late period, at 30 days, the healing processes appeared with small amounts of new woven bone trabeculae present on one side of defect.

In this manuscript, the outcome indicated the formation of immature woven bone that started appearing 15 days after surgery, which was remodelled later to well-developed mature woven bone in the PRF and CSHA. However, the maturation of the bone was significantly higher in the PRF group than in the CSHA group. These differences were related to growth factors within the PRF matrix that can differentiate the MSC into active osteoblasts, stimulate the production of further growth factors from surrounding blood vessels, and promote the osteogenesis process (**Sadek *et al.*, 2023**). PRF results agree with the previous studies that concluded that bone tissue improves with the use of PRF when used in mandibular surgery (**Sharma *et al* ., 2020**).

After seven days in all groups, new bone formation was not observed during histopathological observation. However, new bone formation began at 15 days in all groups except the control group. The control group was filled with fibrous connective tissue with minimal bony fragment formation. In the CSHA group, calcium and phosphate ions were released into the surrounding tissue, which helped regulate the functions of osteoblasts. This process created a local oversaturation of ions, providing more binding sites for cell receptors, which in turn assisted in the adsorption and retention of circulating osteogenic factors like BMPs. These factors ultimately contributed to osteogenesis. (**Polini *et al.*, 2011**). Therefore, the histopathological section of the CSHA group showed a large number of osteoblast cells, especially in the late period.

In the CSHA group, the histopathological section demonstrated a progressive development of new bone with an ossification matrix (**Bigham *et al.*, 2008**). The scaffold's disintegration aids bone regeneration and remodelling by providing a favourable environment for osteoblast differentiation and growth factor production. In the CSHA group, we observed that new bone development occurred progressively. After 15 days, an active, mineralized matrix rich in osteoblast cells started to form. This tissue comprised spicules of woven bone, which were lined by osteoblasts. The spaces between spicules contained loosely arranged stromal and hemopoietic cells. Recent studies suggest that the newly formed bone initiates after implanting the material into the defect site. Gradual degradation by chemical dissolution of ions and cell absorption occurs after implantation in the bone defect. Finally, the newly formed bone tissue replaces the degraded material (**Jasmine, and Krishnamoorthy, 2022**).

The expression mechanisms of ALP are complex, as it plays a critical role in hard tissues such as bone. There are four types of bone tissue expression, namely intestinal ALP, placental ALP, germ cell ALP, and liver/bone/kidney (L, B, and K) ALP, which is called tissue nonspecific alkaline phosphatase (**Sterner *et al.*, 2018**). Alkaline phosphatase is an indicator of progenitor or maturing osteoblasts (**Naji *et al.*, 2022**). Positive alkaline phosphatase immunostaining was observed in some osteoblasts that were lining the trabecular bone. Additionally, during the maturation of a bone bridge on day 30 after a bone defect, some bone bridge lining cells expressed alkaline phosphatase (**Sharma *et al.*, 2014**).

In the control group at 30 days PS, the immunohistochemistry results indicated very weak ALP expression related to the granulocytes in the connective tissue. While in the CSHA group, we found a moderately positive expression of ALP activity. These results are considered with another study that proved the ALP function may require large amounts of extracellular calcium and phosphate. Thus, the presence of hydroxyapatite can enhance ALP activity (**Xian *et al.*, 2004**). Other studies suggested that the positive expression of ALP phosphatase in the bone defects treated with calcium phosphate-based biomaterials was considered an inductive material for ALP activity (**Vimalraj, 2020).**

In group PFR, the positive expression of ALP was considered, with another worker demonstrating that the PRF matrix can increase the expression of osteocalcin in osteoblasts, stimulate osteoblast

proliferation and finally increase the expression of ALP (**Nugraha *et al.*, 2018**), indicating that PRF can promote osteogenic proliferation and differentiation. Consequently, we agree with the previous work that clarified that the PRF matrix has been shown to be highly biocompatible and does not cause cell apoptosis or death (**Wang *et al.*, 2018**).

CONCLUSION

The use of both fabricated CSHA and prepared PRF in the activation healing process of an induced mandible bone defect and the superiority of the beneficial value of using PRF in the histopathological and immunohistchestry assessment emphasis these results.

Conflicts of interest

All authors declare that they have no conflict of interest.

REFERENCES

ABDULGHANI, S., and MITCHELL, G.R., 2019. Biomaterials for in situ tissue regeneration: A review. Biomolecules., 19,9(11):750. https://doi.org/10.3390/biom9110750

ALAM, K., AL-GHAITHI, A., PIYA, S., and SALEEM, A., 2019. In-vitro experimental study of histopathology of bone in vibrational drilling. Medical engineering and physics, 67, 78-87. https://doi.org/10.1016/j.medengphy.2019.03.013

ALKATTAN, L.M., and HELALl, M., 2013. Effects of ketamine-xylazine and propofol-halothane anesthetic protocols on blood gases and some anesthetic parameters in dogs. Veterinary World, 6(2):95-99. http://dx.doi.org/10.5455/vetworld.2013.95-99

ALLAWI, A.H., ALKATTAN, L.A., and AL IRAQI. O.M., 2019. Clinical and ultrasonographic study of using autogenous venous graft and platelet-rich plasma for repairing Achilles tendon rupture in dogs. Iraqi Journal of Vetrinary Science. 33(2):453-460. https://doi.org/10.33899/ijvs.2019.163199

ATIAH, A. 2018. Use of eggshell hydroxyapatite implant in repair of radial bone defects in rabbits . [master's thesis]. Baghdad: University of Baghdad; pp:34.

BIGHAM, A., DEHGHANI, S., SHAFIEI, Z., and TORABI N.S., 2008. Xenogenic demineralized bone matrix and fresh autogenous cortical bone effects on experimental bone healing: radiological, histopathological and biomechanical evaluation. Journal of Orthopedic. Traumatol., 9(2):73-80. https://doi.org/10.1007/s10195-008-0006-6

CHANDRAN, P., and SIVADASB, A., 2014. Platelet-rich fibrin: Its role in periodontal regeneration. Saudi Journal for Dental Research.,5(2):117-122. https://doi.org/10.1016/j.ksujds.2013.09.001

CINTI, F., ROSSANESE, M., BURACCO, P., PISANI, G., VALLEFUCO, R., MASSARI, F., and CANTATORE, M., 2021. Complications between ventral and lateral approach for mandibular and sublingual sialoadenectomy in dogs with sialocele. Veterinary Surgery., 50(3):579-587. https://doi.org/10.1111/vsu.13601

FELIPE R.S., BRUNO, W.M., SIDNEY, W.G.S., IVIA, de P.C., PEDRO, P.R., JOSE, S.C.J., MARIO, T.J., and LUIS, G.G., 2020. Caprine demineralized bone matrix (DBMc) in the repair of non-critical bone defects in rabbit tibias. A new bone xenograft Acta Cirurigca Brasilia .,35(8). https://doi.org/10.1590/s0102-865020200080000001

GAO, C., PENG, S., FENG, P., and SHUAI, C., 2017. Bone biomaterials and interactions with stem cells. Bone research, 5:1-33. https://doi.org/10.1038/boneres.2017.59

GOBBI, G., and VITALE, M., 2012. Platelet-rich plasma preparations for biological therapy: applications and limits. Operative Techniques in Orthopaedics.,22:10-15. https://doi.org/10.1053/j.oto.2012.01.002

HUSSEIN, A.A., and TAQA, G.A., 2021. The impact of natural calcium carbonate and Ubiquinone on bone mineral density in rabbits. Journal of Applied Veterinary Sciences, 6(4):15-22. https://doi.org/10.21608/javs.2021.87062.1091

HAUGEN,H.J., LYUYNGSTADAAS, S.P, ROSSI, F.and GIUSEPPE, P., 2019. Bone grafts: which is the ideal biomaterial?. Clinical Periodontol.,46 Suppl 21:92-102. https://doi.org/10.1111/jcpe.13058

HOSHI, K., AMIZUKA, N., ODA, K., IKEHARA, Y., and OZAWA, H., 1997. Immunolocalization of tissue non-specific alkaline phosphatase in mice. Histochem Cell Biol., 107, 183–191. https://doi.org/10.1007/s004180050103

HUH, J.Y., CHOIi, B.H., KIM, B.Y., LEE, S.H., ZHU, S.J., and JUNG, J.H., 2005. Critical size defect in the canine mandible. Oral Surgery, Oral Medicine, Oral Pathology, Oral Radiologyand Endodontology.,100(3):296-301. https://doi.org/10.1016/j.tripleo.2004.12.015

JASMINE, S., and KRISHNAMOORTHY, R., 2022. Biodegradable Materials for Bone Defect Repair. Biodegradable Materials and Their Applications, 457-470 . https://doi.org/10.1186/s40779-020-00280-6

JIN,Y.H., BYUNG-Ho, C., BYUNG, Y.K, SEOUNG-Ho Lee, and SHI-J.Z,JAE-H.J., 2005. Critical size defect in the canine mandible. Oral Surg Oral Med Oral Pathol Oral Radiol. Endod., 100(3), 0–301. https://doi.org/10.1016/j.tripleo.2004.12.015

KALANTAR, A., and KHORVASH, B., 2006. Repair of skin covering osteoradionecrosis of the mandible with the fas-ciocutaneous supraclavicular artery island ap: case re- port. J.J Cranio Maxillo Facial Surgery ., 34(7):440-2 https://doi.org/10.1016/j.jcms.2005.05.006

KOMATSU, D.E., BRUNE, K.A., LIU, H., SCHMIDT, A.L., HAN, B., ZENG, Q.Q., and GEISER, A.G., 2009. Longitudinal in vivo analysis of the region-specific efficacy of parathyroid hormone in a rat cortical defect model. Endocrinology, 150(4): 1570-1579. https://doi.org/10.1210/en.2008-0814

MAREI, H.F, MOHMOOD, K., and ALMAS, K., F.D.S. (RCSEd)., 2017. Critical Size Defects for Bone Regeneration Experiments in the Dog Mandible: A Systematic Review .Implant Dintersry ., 27(1). https://doi.org/10.1097/id.0000000000000713

MOHAMMED, F.M., ALKATTAN, L.M., AHMED, M.S., and THANOON M.G., 2023. Evaluation the

effect of high and low viscosity Nano-hydroxylapatite gel in repairing of an induced critical-size tibial bone defect in dogs: Radiolographical study. Journal of Applied Veterinary Sciences,8(3):105-110. https://dx.doi.org/10.21608/javs.2023.215990.1239

MOHAMMED, F.M., ALKATTAN, L., and M.ISMAIL, H.K., 2022. Histopathological and serological assessment of using rib lamb xenograft reinforced with and without hydroxyapatite nano gel for reconstruction tibial bone defect in dogs. Iraqi Journal of Vetrinary. Science, 36, Supplement I, (69-76). https://doi.org/10.33899/ijvs.2022.135366.2473

NAJI, A.H., Al-WATTAR, W.T., and TAQA, G.A., 2022. The Effect of Xylitol on Bone Alkaline Phosphatase Serum Level and Bone Defect Diameter in Rabbits. Journal of Applied Veterinary Sciences, 7(1), 6. https://dx.doi.org/10.21608/javs.2021.97815.1105

NUGRHA, A.P., NARMADA, I.B., ERNAWATI, D.S., DINARYANTI, A., HENDRIANTO, E., RIAWAN, W., and RANTAM, F.A., 2018. Bone alkaline phosphatase and osteocalcin expression of rat's Gingival mesenchymal stem cells cultured in platelet-rich fibrin for bone remodeling (in vitro study). European Journal Dent.,12(04), 566-573. https://doi.org/10.4103/ejd.ejd_261_18

POLINI, A., PISIGNANO, D., PARODI, M., QUARTO, R., and SCAGLIONE, S., 2011. Osteoinduction of human mesenchymal stem cells by bioactive composite scaffolds without supplemental osteogenic growth factors. Plos one, 6(10), e26211. https://doi.org/10.1371/journal.pone.0026211

ROUDANA, M.A., RAMESHA, S.,NIAKANB, A.,WONGA, Y.H., ZAVAREHA, M.A., CHANDRANC, H., and SUTHARSINIF, U., 2017. Thermal phase stability and properties of hydroxyapatite derived from bio-waste eggshells. Journal of Ceramic Processing Research., 18(1): 69.

SADEK, A.A., ABD-ELKAREEM, M., ADBELHAMID, H.N., MOUSTAFA, S., and HUSSEIN, K., 2023. Repair of critical-sized bone defects in rabbit femurs using graphitic carbon nitride (g-C3N4) and graphene oxide (GO) nanomaterials. Scientific Reports, 13(1):5404. https://doi.org/10.1038/s41598-023-32487-7

SHADJOU, N., and HASANZADEH, M., 2015. Bone tissue engineering using silica-based mesoporous nanobiomaterials: Recent progress. Materials Science and Engineering., 55:401-409. https://doi.org/10.1016/j.msec.2015.05.027

SHARMA, A., INGOLE, S., DESHPANDE, M., RANADIVE, P., SHARMA, S., KAZI, N., and RAJURKAR, S., 2020. Influence of platelet-rich fibrin on wound healing and bone regeneration after tooth extraction: A clinical and radiographic study. J Oral Biol Craniofac Research , 10(4): 385-390. https://doi.org/10.1016/j.jobcr.2020.06.012

SHARMA, U., PAL, D., and PEASAD, R., 2014. Alkaline phosphatase: an overview. Indian Journal Clinical Biochemical., 29: 269-278. https://doi.org/10.1007%2Fs12291-013-0408-y

STERNER, R.M., KREMER, K.N., DUDAKOVIC, A., WESTENDROF, J.J., VAN WIJNEN, A.J., and HEDIN, K. E., 2018. Tissue-Nonspecific Alkaline Phosphatase Is Required for MC3T3 Osteoblast–Mediated Protection of Acute Myeloid Leukemia Cells from Apoptosis. The Journal .of Immunology., 201(3):1086-1096. https://doi.org/10.4049/jimmunol.1800174

SURVANA, S.K., LAYTON, C., BANCROFT, J.D., and BANCROF S., 2013 . Theory and Practice of Histological Techniques.7th ed. Churchill Livingstone Press ,USA. P. 12-32 .

TAMBELLA, A.M, BARTOCETTI,F., ROSSI, G, GALOSI, L., CATONE,G., FALCONE,A., and VULLO, C., 2020. Effects of Autologous Platelet-Rich Fibrin in Post-Extraction Alveolar Sockets: A Randomized, Controlled Split-Mouth Trial in Dogs with Spontaneous Periodontal Disease. Animals, 10(8):1343. https://doi.org/10.3390/ani10081343

VIMALRAJ, S. 2020. Alkaline phosphatase: Structure, expression and its function in bone mineralization. Gene, 754:144855.

WANG, X., ZHANG, Y., CHOUKROUM, J., GHANAATI, S., and MIRON, R.J., 2018. Effects of an injectable platelet-rich fibrin on osteoblast behavior and bone tissue formation in comparison to platelet-rich plasma. Platelets, 29(1):48-55. https://doi.org/10.1080/09537104.2017.1293807

XIAN, C.J., ZHOU, F.H., MCCARTY, R.C., and FOSTER, B.K., 2004. Intramembranous ossification mechanism for bone bridge formation at the growth plate cartilage injury site. Journal of Orthopedic Research ., 22(2):417-426 . https://doi.org/10.1016/j.orthres.2003.08.003

ZEBON, S.H., EESA, M.J., and BAHAA,,F.H., 2020. Efficacy of Nano Composite Porous 3D Scaffold of Crab Shell and Al-Kharit,Histological and Radiological for Bone Repair in Vivo. Iraq Jounal of Veterinary. Medicine., 44(2),15–24. https://doi.org/10.30539/ijvm.v44i2.973

ZEDAN, I.A., ALKATTAN, L.A., AL IRAQI, O.M., 2022. An evaluation of Aloe vera leaves gel with polypropylene mesh to repair of ventrolateral abdominal hernia in rams . Iraqi Journal. Vetrinary. Science., 36:19-25. .

ZEDAN, I.A., ALKATTAN, L.A., and Al-MAHMOOD, S.S., 2023. Histopathological and immunohistochemical assessment of the using platelets rich fibrin to reinforce ventral hernioplasty in the sheep modelIraqi . Iraqi Journal. Vetrinary. Science .,37, (4): 821https://www.vetmedmosul.com/article_180501.html

ZHANG, Q., WU, W., QIAN, C., XIAO, W., ZHU, H., and GUO,J.,CUI,W., 2019. Advanced biomaterials for repairing and reconstruction of mandibular defects. Materials Science and Engineering.,103:109858.

How to cite this article:
Ali Ghazi Atiyah[1] and Alkattan L.M., 2024. Impact of Fabricated Coral Shell Hydroxyapatite Powder and Autologous Plasma Rich- fibrin in Remodeling of the Mandibular Bone Critical Size Defect in Dogs: Histopathological and Immunohistochemical Study. Journal of Applied Veterinary Sciences, 9 (2): 111-119.
https://dx.doi.org/10.21608/javs.2024.266431.1312